Applied Surface Science 431 (2018) 160–164

Contents lists available at ScienceDirect

Applied Surface Science

journal homepage: www.elsevier.com/locate/apsusc

Full Length Article

Influence of hysteresis effect on properties of reactively sputtered TiAlSiN films

Fangyuan Gao[a,b], Guang Li[a,b], Yuan Xia[a,b,*]

[a] Institute of mechanics, Chinese Academy of Sciences, Beijing 100190, China
[b] University of Chinese Academy of Sciences, Beijing 100049, China

ARTICLE INFO

Article history:
Received 22 January 2017
Received in revised form 16 July 2017
Accepted 30 July 2017
Available online 16 August 2017

Keywords:
TiAlSiN films
Reactive sputtering
Hysteresis effect
Plasma characteristics
Mechanical properties

ABSTRACT

This article reports on the hysteresis effect in TiAlSiN films prepared by an intermediate frequency magnetron. The discharge voltages for different metallic alloy targets varying with nitrogen flow rate were systematically investigated, under a constant pressure provided by sputtering gas. The hysteresis transition was introduced by the sudden changes in sputtering rate, fraction of compound formation, phase composition and mechanical properties. The result was shown that: the initial growth rate a_D in metallic mode was 4 times faster than that in supersaturated state. The optimized stoichiometric TiAl(Si)$N_{x=1}$ films containing 50 at.% N were founded in the transition region. The discussion on the plasma characteristics caused by hysteresis process showed that the TiN(111) texture could be increased by applying higher particle bombarding energy. The hardness of TiAlSiN film was strongly influenced by the orientation, which depended on the loading history of nitrogen. The superior TiAlSiN film with hardness 33 GPa could be prepared during the nitrogen unloading for same nitrogen flow rates.

1. Introduction

In the last decades, titanium nitride (TiN) has been used as wear and corrosion protective coating to enhance the lifetime and performance of cutting tools. While, titanium aluminium nitride (TiAlN) coatings are preferred alternative to TiN due to the excellent high temperature oxidation resistance [1,2]. For the increasing requirements on high speed and dry cutting applications at elevated temperatures, further researches of titanium aluminium silicon nitride (TiAlSiN) are of great importance. The incorporation of hard nanocrystalline TiAlN phases with improved oxidation resistance, and Si_3N_4 amorphous phase achieving superhardness, has allowed increasing the hardness as well as thermal stability [3,4]. Many studies [5–7] have shown that the superior properties of the TiAlSiN films are attributed to the particular dispersion strengthening structure. Therefore, it is important to achieve control of the film structure, and ensure the repeatability of the production process.

Hysteresis effect is a well-known and important feature of reactive magnetron sputtering. Depending on the amount of reactive gas used in the film deposition, the reactive sputtering process can be divided into three modes: (a) metallic, (b) transition and (c) reactive [8–10]. The target sputtering and film deposition process however depends strongly not just on the flow of reaction gas, but also on the history of the gas use, namely, loading or unloading. Hence, reactive sputtering exhibits quite complex processing behavior when flow control of reactive gas is used [11–14]. In other words, it is practically possible that exactly the same experimental parameters, but different film structure and properties, just because the loading history of the reaction gas is not the same. Therefore, it appears that there is a need to explore the characteristics of target sputtering and its responses on the plasma parameters, in order to establish a process map of ideal working conditions for the optimal structure and performance.

In this study, the hysteresis effect under a constant total pressure of sputtering gas for different reactive gas flow rates, in the reactive magnetron sputtering process of TiAlSiN films has been systematically investigated. The main aim of this study is to find the influence of hysteresis effect on target voltage, plasma parameters and the correlations between deposition rate, chemical composition, structure, and mechanical properties of the thin films and is therefore vital for manufacturing processes.

2. Experimental

TiN, AlN, TiAlN and TiAlSiN films were reactively sputter deposited in a mixture of Ar and N_2 using an unbalance intermediate frequency magnetron equipped, from commercial targets: pure Ti, Al (99.999% purity) and alloyed AlSi (90/10 at.%) of 80 mm

* Corresponding author at: No.15 Beisihuanxi Road, Institute of Mechanics, Chinese Academy of Sciences, Beijing 100190, China.
E-mail addresses: gaofangyuan@imech.ac.cn (F. Gao), lghit@imech.ac.cn (G. Li), xia@imech.ac.cn (Y. Xia).

http://dx.doi.org/10.1016/j.apsusc.2017.07.283
0169-4332/

Table 1
Deposition conditions for TiN, AlN, TiAlN, TiAlSiN films by an intermediate frequency magnetron sputtering system.

Reactive gas		Ar 20 sccm N_2 0–20 sccm
Base pressure		1.0×10^{-3} Pa
Working pressure		5.0×10^{-1} Pa
Sputtering target	TiN	1 × Ti (99.999%)
	AlN	1 × Al (99.999%)
	TiAlN	1/2 × Ti (99.999%) + 1/2 × Al (99.999%)
	TiAlSiN	1/2 × Ti (99.999%) + 1/2 × AlSi (90/10 at.%)
Target current		0.5A
Substrate bias		−150 V
Rotational velocity		3 rpm
Distance (substrate to target)		100 mm
Deposition temperature		Room temperature (without heating)

in diameter. The metal targets were cut apart and combined into a round planar target that can interact with nitrogen gas to form different films.

A rotating sample holder was located at the center of the chamber. The films were deposited on polished and ultrasonically cleaned Si wafers. After loading, the vacuum chamber was evacuated to a base pressure of 1.0×10^{-3} Pa. This was followed by argon-hydrogen plasma cleaning under an operating pressure of 1.5 Pa for 10 min at a discharge voltage of −900 V, which helps to remove the oxide layer effectively from the substrates. Detailed deposition process conditions are shown in Table 1. The total sputtering gas pressure was kept constant at 5.0×10^{-1} Pa by adjusting the vacuum chamber flapper valve.

In the process of loading or unloading nitrogen, every increase or decrease of gas flow, it is necessary to confirm that the voltage in 20 min is stable and free of fluctuation. A dynamic equilibrium is formed at the target surface, which could be used to record the parameters of hysteresis curves or to prepare the coatings. The thickness of all the films was controlled to approximately 2.5 μm.

Plasma characterization was made by a cylindrical Langmuir probe, consisting of a tungsten wire of length $l_{pr} = 5.0 \pm 0.5$ mm and diameter $r_{pr} = 0.20 \pm 0.01$ mm. The probe holder was an alumina tube with an outer radius $r_{prh} = 0.5$ mm and a length $l_{prh} = 20$ mm. The probe was positioned at 100 mm from the target along the target-axis. The Langmuir probe current was determined by measuring the voltage over a resistor (10 Ω). The probe current and voltage were then collected and stored in a computer for later analysis.

The film thickness was investigated by using a high resolution field emission scanning electron microscope (FESEM). The chemical composition of the films was determined by energy dispersive X-ray spectrometry (EDXS) using an S-570 SEM equipped. The crystal structure and phase of the coatings were identified by glancing-angle X-ray diffraction (XRD) with Cu Kα radiation (50 kV, 100 mA). The hardness measurements of the coatings were performed by using a nanoindenter (CSM instruments) that employed a Berkovich diamond indenter. Each sample was made of ten indentations and the value of the hardness reported here is the average of the ten measured values and the maximum indentation depth was restricted to one-tenth thickness of the coatings to minimize the effect of substrate on the hardness measurement.

3. Results

3.1. Hysteresis effect

The experimental dependences of the discharge voltage on nitrogen flow rate for different target materials are depicted in Fig. 1. As seen in this figure, for the metallic nitride TiN curve, the target voltage increases with increasing reactive gas flow rate.

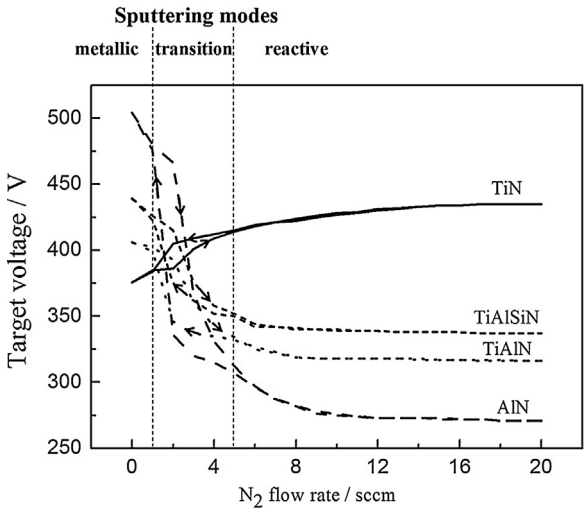

Fig. 1. Measured target voltage for different metallic alloy targets as a function of nitrogen flow rate.

In contrast, the target voltage decreases sharply when aluminium or silicon is added as the target materials. The discharge voltage increases or decreases depending on a decreased or increased secondary electron emission coefficient of the nitrided target surface [15–17]. The secondary electron emission yields from different compounds depend on their electronic properties, such as the metallic nitrides TiN, and the insulating nitrides AlN and Si_3N_4. The TiN compound formation on the target surface gradually increases the voltage due to lower secondary electron emission, while AlN and Si_3N_4 decrease the voltages under a higher yield of secondary electrons.

Obviously, the data demonstrates a typical track of target voltage indicating that hysteresis phenomenon. In the case of TiAlSiN, the target voltage initially decreases as the reactive gas flow rate is increased, but there is a sharp decrease in the target voltage which is the point that the target becomes poisoned. When the gas flow rate is reduced, the target voltage remains low until the compound layer on the target surface is broken through and then the cathode voltage returns the higher values corresponding to the metallic deposition mode. Then, a closed hysteresis loop is formed. And it is observed that, in the process of N_2 increased and decreased, the target voltages show significant differences in the same flow rate at the transition region.

3.2. Deposition rate

The deposition rates a_D of the TiAlSiN films is given as a function of the reactive gas flow rate in Fig. 2. It can be seen that a_D of the films sputtered in the metallic mode is 4 times higher than that of films sputtered in the reactive mode. A strong decrease of a_D in the transition mode is caused by the Ti/AlSi target poisoning, by covering of the target surface with TiAlSiN nitride.

The deposition rate in hysteresis process is consistent with the variation of target voltage. The experimental conditions are exactly the same, but the different adding processes of reactive gas, the growth rate a_D of the films will have certain diversity. When the reactive gas nitrogen increased to the saturation and then decreased, the film growth rates are lower than the simple load.

3.3. Phase composition

The structure of the TiAlSiN film can be easily controlled by reactive gas flow rate. In other words, the content of N elements in the

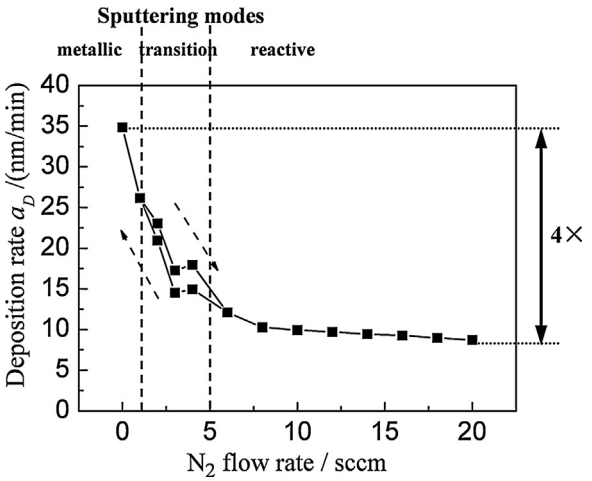

Fig. 2. Deposition rate of the TiAlSiN films during their growth as a function of nitrogen flow rate.

film determines what crystal phase is formed. A development of the structure of TiAlSiN films sputtered with increasing gas flow rate is given in Fig. 3. Here, for a simplicity of explanation the values of nanohardness H, stoichiometry $x = N/(Ti + Al + Si)$ and Si element content are also given. The XRD patterns mainly show the diffraction peaks of TiN and AlN crystal phase. This result implied that Si is present in an amorphous Si_3N_4 matrix phase around the TiAl(Si)N crystallites. This would confirm the results of other recent investigations by XPS analysis [18–21].

The film sputtered at $F_{N2} = 0$ sccm is a pure TiAlSi film. With increasing F_{N2} the film gradually varies from a solid solution Ti(AlSi)N through a tetragonal Ti_2N phase at approximately 26 at.% N ($x = 0.35$) to a cubic TiN phase. From Fig. 3 it is seen that inside the transition mode of sputtering, with increasing F_{N2} the diffraction peak intensity of crystal plane (111) gradually increases. There is a transition region which separates TiAlSiN films with a strong (200) preferred orientation on side of lower F_{N2} from those with no visible preferred orientation on side of higher F_{N2}.

A typical development of the elemental composition of TiAlSiN films with increasing gas flow rate F_{N2}. It shows that the nitrogen content in the TiAlSiN films increases with increasing F_{N2} and already at $F_{N2} = 3$ sccm the amount of N in the film achieves 50 at.%. The stoichiometric TiAl(Si)$N_{x=1}$ nitride films with $x = N/(Ti + Al + Si)$ are formed in the transition mode and a_D of these films is higher than that of overstoichiometric ($x > 1$) nitride films produced in the nitride mode.

3.4. Mechanical properties

Mechanical properties of hard TiAlSiN films are well described by their nanohardness H in Fig. 4. In order to facilitate the discussion, the gas flow rate F_{N2} is defined as (+) in the loading process, corresponding as (−) in the unloading process. It can be seen that, the film hardness has a significant increase with the supply of reactive gas nitrogen. In the transition region, the hardness of the films with increasing nitrogen flow rate is further increased, and reaches

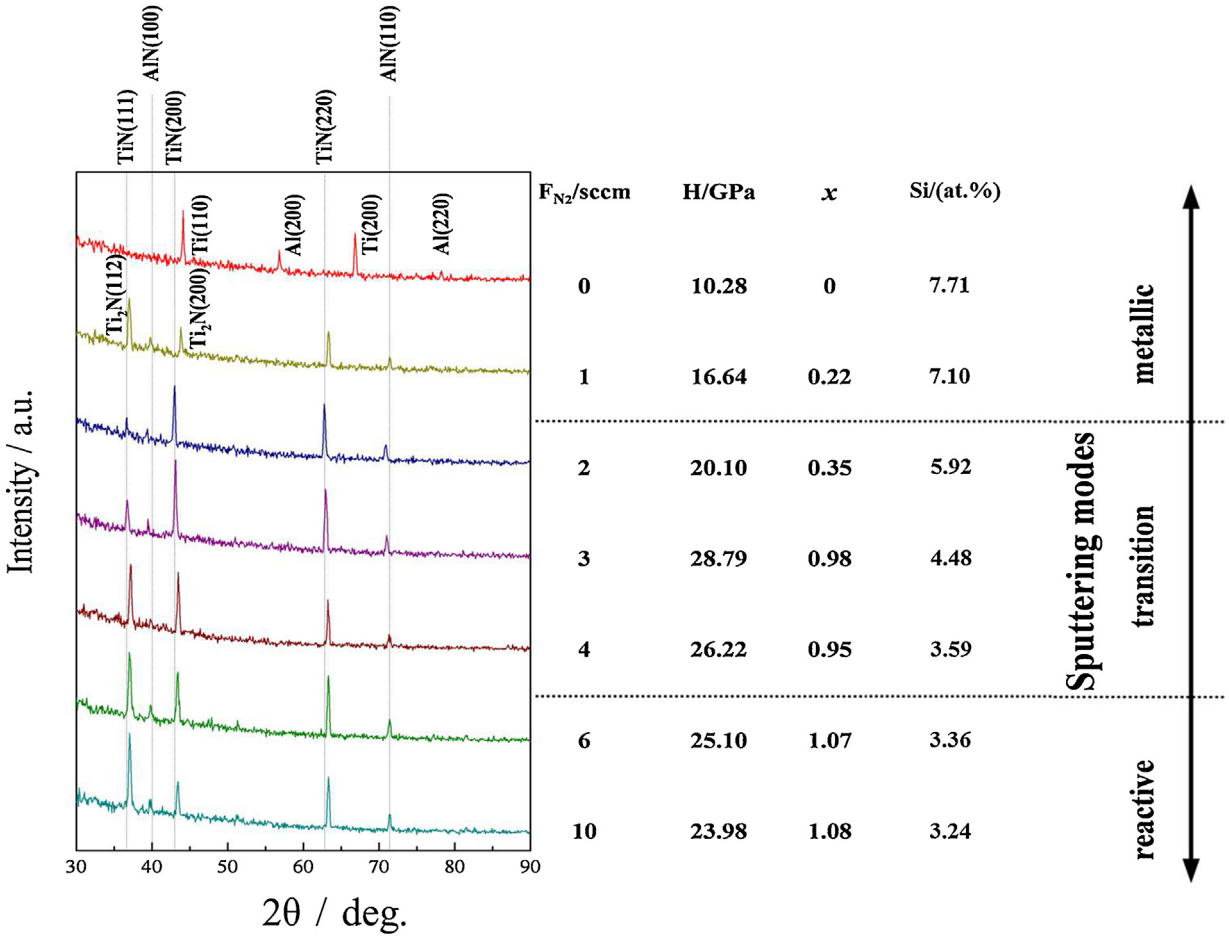

Fig. 3. XRD patterns from TiAlSiN films as a function of the increased nitrogen flow rate in the loading process.

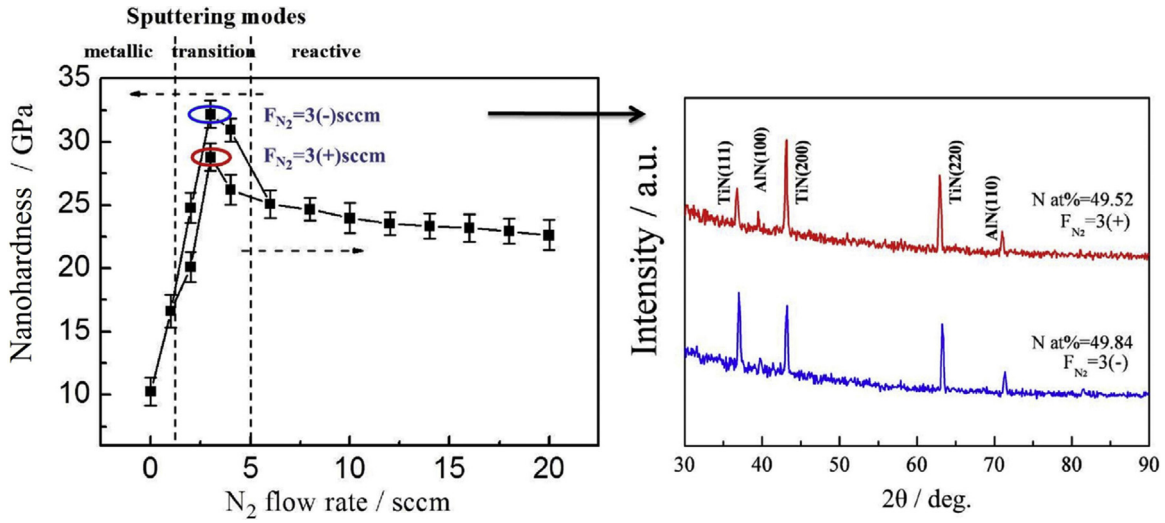

Fig. 4. Nanohardness of reactively sputtered TiAlSiN films as a function of nitrogen flow rate.

a maximum at the F_{N2} = 3(+) sccm. When the gas increased to the saturation state, the film hardness decreases under the increasing nitrogen flow rate, but the change in amplitude is small and stabilized. In addition, comparing with the simple loading process in transitional mode, the hardness of TiAlSiN films prepared in unloading process improves significantly, and the highest hardness value 33 GPa is obtained at the F_{N2} = 3(−) sccm.

Further analysis revealed, the differences in XRD patterns of TiAlSiN films prepared in loading or unloading process are obvious under the same nitrogen flow rate (F_{N2} = 3 sccm). Compared with the simple loading process, the diffraction intensity of the peak (111) for nitride crystalline phase increases conspicuously in unloading, the peak (200) decreased, while the peak (220) changes little.

4. Discussion

As shown in Fig. 4, the TiAlSiN film achieves the highest hardness when the stoichiometry of the nitrogen reaches the optimum 50%. However, at the same stoichiometric ratio, what causes the obviously different on the structure and mechanical properties of the films, under different nitrogen loading and unloading modes.

Dependences of the plasma density and electron temperature of TiAlSiN films as a function of nitrogen flow rate are given in Fig. 5. It can be seen that the plasma parameters as the loading and unloading of reactive gas nitrogen, display the similar tracks with the target voltages. The hysteresis region of the plasma density N_e is obvious because of a difference between sputtering yield from the cleaned part of the target and from the poisoned part of the target. The transition between the metal and the reactive mode is given by newly generated process conditions in the whole reactor when a critical reactive gas flow rate is reached.

From this figure it is seen that electron temperature KT_e is the lowest in the metallic mode, increases in the transition mode and saturates in the reactive mode where achieves a maximum value $KT_{e\max}$. With a further increase in nitrogen flow rate, the collision probability between the electron and gas molecules gradually increases. Because of the energy lose in collisions, the electron temperature decreases in a relatively slow trend. In the unloading process of the reactive gas N_2, the electron temperature is maintained at the higher bit until the gas flow rate reduced to a critical value. Therefore, in the same nitrogen flow rate, the plasma in the transition mode of unloading process can obtain higher electron

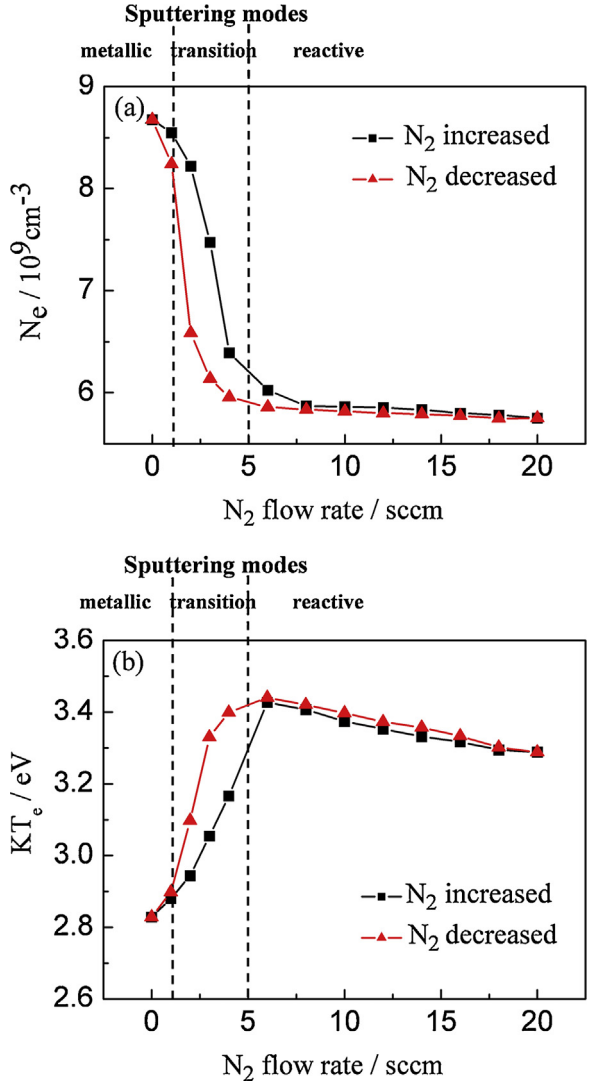

Fig. 5. Measured plasma density (a) and electron temperature (b) as a function of nitrogen flow rate.

temperature than loading, that is, a higher average particle energy distribution.

The particle bombarding energy significantly affects the microstructure and mechanical properties of the films, which delivered to the growing films is proportion to the particle energy distribution. According to the evolution of plasma characteristics in hysteresis process, the higher particle bombarding energy could be gained in the unloading process compared with the loading mode. As shown of the XRD diagrams in Fig. 4, the loading deposition process favors the growth of (200) for TiN. This is in agreement with the theoretical calculation which revealed that (200) planes for TiN have minimum surface energy and thus, favorable directions for the growth of textured films [22]. While under the higher particle bombarding energy, the growth in the plane (111) direction increases significantly. And the higher hardness has been found with the increased TiN(111) texture. It can be attributed to the fact that the (111) plane is the most close-packed surface in the TiN film. The hardness of the film is anisotropic and strongly influenced by the orientation, in which the (111) orientation shows the highest hardness, which is consistent with previous observations [23,24].

Therefore, the structure and properties of the film are the results of the combined effects of physical and chemical processes, are controlled by the energy distribution and elements stoichiometric in the plasma environment.

5. Conclusion

A systematic research on the hysteresis effect in the reactive magnetron sputtering process of TiAlSiN films has been achieved. The result indicates that, with the loading and unloading of nitrogen, the voltages of sputter targets showed the distinct hysteresis effects. Along with the increase of the nitrogen flow, the deposition rate of TiAlSiN film reduced dramatically, and the initial growth rate a_D was 4 times higher than that in supersaturated state. When the flow rate increased to 3 sccm in the transition region, the optimized stoichiometric $TiAl(Si)N_{x=1}$ films containing 50 at.% N were produced. In addition, the TiAlSiN film obtained the highest hardness in the process of nitrogen unloading, about 33 GPa. The effect caused by the hysteresis process, on the target sputtering and plasma characteristics was also discussed. The study showed that, in the same nitrogen flow rate, compared with the loading process, the higher particle bombarding energy was obtained during the unloading. The higher particle bombarding energy increased the growth in the plane (111) direction significantly. The hardness of TiAlSiN film was strongly influenced by the (111) orientation. The superior TiAlSiN films with the highest hardness were prepared during the nitrogen unloading process.

Acknowledgements

This work is financially supported by the International Science & Technology Cooperation Program of China (No.2014DFG51240) and the Strategic Priority Research Program of the Chinese Academy of Sciences (No.XDB22040503).

References

[1] S. Hofmann, H.A. Jehn, Surf. Interf. Anal. 12 (1988) 329.
[2] D. McIntyre, J.E. Greene, G. Hakansson, J.E. Sundgren, W.D. Munz, J. Appl. Phys. 67 (1990) 1542.
[3] S. PalDey, S.C. Deevi, Mater. Sci. Eng. A 342 (2003) 58.
[4] S. Carvalho, L. Rebouta, A. Cavaleiro, L.A. Rocha, J. Gomes, E. Alves, Thin Solid Films 398-399 (2001) 391.
[5] M. Parlinska-Wojtan, A. Karimi, T. Cselle, M. Morstein, Surf. Coat. Technol. 177–178 (2004) 376.
[6] C.L. Chang, J.W. Lee, M.D. Tseng, Thin Solid Films 517 (2009) 5231.
[7] K. Zhang, L.S. Wang, G.H. Yue, Y.Z. Chen, D.L. Peng, Z.B. Qi, Z.C. Wang, Surf. Coat. Technol. 205 (2011) 3588.
[8] J. Musil, P. Baroch, J. Vlcek, K.H. Nam, J.G. Han, Thin Solid Films 475 (2005) 208.
[9] F.G. Cougnon, K. Strijckmans, R. Schelfhout, D. Depla, Surf. Coat. Technol. 294 (2016) 215.
[10] E. Haye, F. Capon, S. Barrat, D. Mangin, J. Pierson, Surf. Coat. Technol. 298 (2016) 39.
[11] W.D. Sproul, D.J. Christie, D.C. Carter, Thin Solid Films 491 (2005) 1.
[12] K. Danisman, S. Danisman, S. Savas, I. Dalkiran, Surf. Coat. Technol. 204 (2009) 610.
[13] E. Särhammar, K. Strijckmans, T. Nyberg, S. Van Steenberge, S. Berg, D. Depla, Surf. Coat. Technol. 232 (2013) 357.
[14] D. Depla, J. Haemers, R. De Gryse, Surf. Coat. Technol. 235 (2013) 62.
[15] R. Mientus, K. Ellmer, Surf. Coat. Technol. 116–119 (1999) 1093.
[16] D. Depla, X.Y. Li, S. Mahieu, R. De Gryse, J. Phys. D: Appl. Phys. 41 (2008) 202003.
[17] M. Arif, C. Eisenmenger-Sittner, Surf. Coat. Technol. 324 (2017) 345.
[18] H.C. Barshilia, M. Ghosh, Shashidhara, R. Ramakrishna, K.S. Rajam, Appl. Surf. Sci. 256 (2010) 6420.
[19] T. Chen, Z.W. Xie, F. Gong, Z.Z. Luo, Z. Yang, Appl. Surf. Sci. 314 (2014) 735.
[20] L.H. Zhu, C. Song, W.Y. Ni, Y.X. Liu, Trans. Nonferrous Met. Soc. China 26 (2016) 1638.
[21] N.R. He, H.X. Li, L. Ji, X.H. Liu, H.D. Zhou, J.M. Chen, Tribol. Int. 98 (2016) 133.
[22] D.R. Mckenzie, Y. Tin, W.D. Mcfall, N.H. Hoang, J. Phys. Condens. Matter 8 (1996) 5883.
[23] C.T. Chen, Y.C. Song, G.P. Yu, J.H. Huang, J. Mater. Eng. Perform. 7 (1998) 324.
[24] J.H. Huang, Y.P. Tsai, G.P. Yu, Thin Solid Films 355–356 (1999) 440.